

# Tunable coupled quantum dots formed by local implantation of arsenic donors in a silicon nanowire.

M. Pierre,<sup>1</sup> R. Wacquez,<sup>1</sup> B. Roche,<sup>1</sup> X. Jehl,<sup>1</sup> M. Sanquer,<sup>1, a)</sup> and M. Vinet<sup>2</sup>

<sup>1)</sup> CEA-DSM-INAC-SPSMS, 38054 Grenoble, France

<sup>2)</sup> CEA/LETI-MINATEC, 38054 Grenoble, France

(Dated: 22 February 2019)

Tunable coupled quantum dots have been made by local arsenic implantation in a silicon nanowire. Two doping levels are obtained using gates and nitride spacers as blanket masks sequentially during implantation. The in-and-out tunneling rates towards low resistive electrodes and the coupling between dots can be tuned independently using strongly coupled control top gates which wrap the silicon nanowire.

Versatile silicon quantum dots can be achieved by using a combination of implantation and local top gates. Recently we have made compact coupled MOS-SETs<sup>1</sup> (Metal-Oxide-Semiconductor Single Electron Transistor) which are defined by two accumulation 2DEG quantum dots below the gates and isolated from electrodes by non-intentionally doped silicon nanowires below nitride spacers<sup>2</sup>. MOS-SETs can be used to sense the position, spin and ionization state (in real time) of nearby implanted single donors<sup>3</sup>.

In this work we use arsenic (As) implantation to fabricate compact coupled dots which are separated by tunable tunnel barriers. To achieve this goal we use Lightly Doped Drain (LDD) implantation of As below the spacers (see Fig. 1c). This implantation tunes the conductance of the access regions to the channel so that the MOS-SET effect below the top gate does not occur at low temperature as in Ref. 1 (see Fig. 1b). As a result top gates control the transmission of undoped nanowires on both sides of an As doped Coulomb island. Finally using three gates in series a fully tunable implanted double dot is realized.

Gate-controlled tunneling to electrodes in silicon coupled dots has previously only been demonstrated in intrinsic silicon<sup>4</sup>. Coupled dots designed by phosphorous implantation in bulk crystal have no full control of tunnel barriers to electrodes<sup>5–7</sup>. Our implanted quantum dot (resp. coupled dots) are very similar to those presented in Refs. 4, 8, 9 (resp. 4, 10) but without the upper gate which is replaced by local As doping. The advantage of doped quantum dots is the large density of carriers, which enables strong screening of the disorder potential, together with a sharp and fixed confinement potential. The lateral gradient for dopant concentration achieved here with our state-of-the-art CMOS implantation and annealing process is typically one order of magnitude in concentration every 5 nm. Replacing the second upper gate layer by donor implantation also reduces the number of input voltage variables, cross talking and parasitic capacitances. With an atomistic control local implantation is also particularly attractive with the perspective of the single dopant limit<sup>3,11–16</sup>.

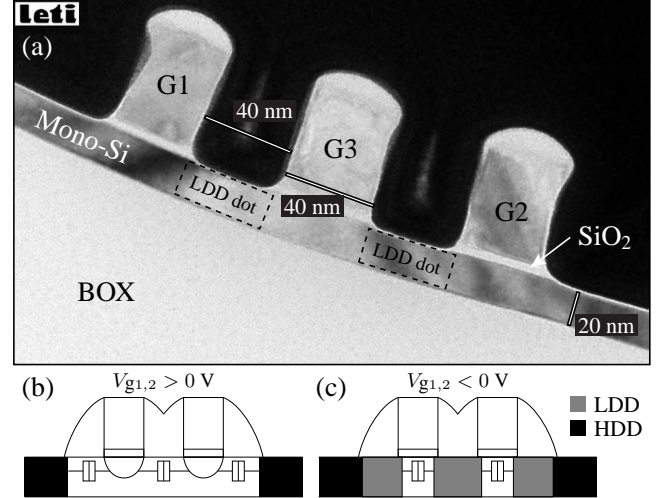


FIG. 1. (a) TEM micrograph of a typical triple gate sample before spacer formation. The gate length is 40 nm and the spacing between gates is 40 nm. (b) Schematic of a double gate sample without LDD. A double dot is created by accumulation of carriers below the two gates<sup>1</sup>. (c) Schematic of a double gate sample with LDD. A dot is created by implantation of Arsenic dopants between the gates. Its coupling to the electrodes is tuned by the two top gates (see Figs. 3 and 4).

Our samples are produced on 200 mm silicon-on-insulator (SOI) wafers in a CMOS platform. Many samples have been built and measured. The results and conclusions presented are valid for most of these samples. A 200 nm long, 20 nm thick and 60 nm wide silicon nanowire is etched and covered by two or three  $L_g = 40$ –60 nm long polysilicon gates which are isolated by 5 nm thick  $\text{SiO}_2$  gate oxide (Fig. 1). The spacing between gates is  $L_{gg} = 40$  nm. 40 nm thick silicon nitride spacers are formed on both sides of the gates. The only difference with samples described in Ref. 1 relies on the LDD doping which is performed after gate and before spacers formation. All the data that are presented are for samples with LDD except in Fig. 2 as noted. The LDD doping of the SOI is  $5 \times 10^{13} \text{ cm}^{-2}$ . The number of As atoms in the central region between the gates is about

<sup>a)</sup> marc.sanquer@cea.fr

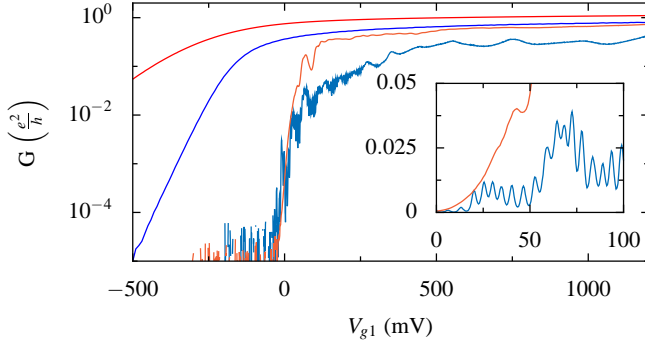


FIG. 2. Drain-source conductance of two double gate samples versus  $V_{g1}$  at room temperature and 4.2 K.  $V_{g2} = 1.2$  V, thus conductance is determined by the region below gate 1. Blue curves: sample without LDD and with  $L_g = 60$  nm. Regular CBO are observed at 4.2 K due to the formation of a dot<sup>1,2</sup> below gate 1 and tunneling of electrons through the undoped nanowires located below the spacers (see Fig. 1b). Red curves: sample with LDD and  $L_g = 50$  nm. No CBO is observed (see Fig. 1c). Inset: detail at 4.2 K in linear scale.

1200 ( $5 \times 10^{13} \text{ cm}^{-2} \times 40 \text{ nm} \times 60 \text{ nm}$ ). Highly Doped Drain (HDD) implantation is performed after spacer deposition using As at  $2 \times 10^{15} \text{ cm}^{-2}$ . The thick spacers protect the central region from HDD doping.

In samples without LDD implantation the undoped regions below the spacers become insulating at low temperature, resulting in the formation of a dot below the gate<sup>1,2</sup>. In contrast confinement of carriers in the channel does not occur when the access regions are doped, this can be seen on Fig. 2. The conductance of two-gate samples is shown as a function of  $V_{g1}$ , while  $V_{g2}$  is kept at a large positive value (1.2 V). The conductance is therefore controlled by  $V_{g1}$ , as the channel below gate 2 only acts as a smaller constant series resistance. When the access regions are undoped clear regular Coulomb blockade oscillations (CBO) are seen at 4.2 K, i.e. a MOS-SET exists below gate 1, whereas only aperiodic structure is observed after LDD doping. In both cases the aperiodic conductance fluctuation observed at low temperature, either modulated by CBO or not, is sample-specific and is due to the static disorder in the silicon nanowire below the spacers<sup>3</sup> which is not screened because of the low density of carriers in these regions.

CBO are restored in samples with LDD only when *both* gate voltages  $V_{g1}$  and  $V_{g2}$  are a few hundred millivolts above the onset of the current, which depends on the gate length (see Figs. 3 and 4). Larger negative  $V_g$  are necessary to deplete the nanowire below the shortest gates which contains some As donors laterally diffused from LDD. The period of CBO is very regular and identical for both samples whatever the onset voltage. This reflects the fact that the Coulomb island is LDD doped and contains a high density of electrons irrespective of  $V_{g1}$  and  $V_{g2}$ , the one-particle mean-level spacing being thus negligible. The period of CBO is approx. 10 mV in

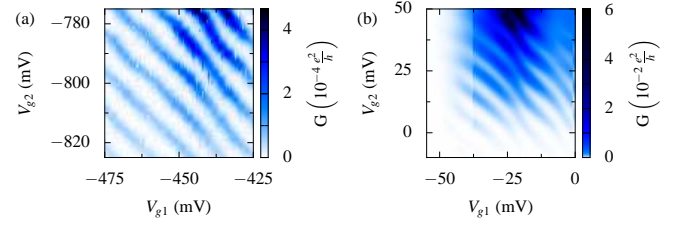


FIG. 3. Color plot of the drain-source conductance versus  $V_{g1}$  and  $V_{g2}$  at 4.2 K. CBO are periodic in  $(V_{g1} + V_{g2})$ . (a) (resp. (b)) sample with  $L_g = 50$  nm (resp. 60 nm). Therefore the onset of the current is at different gate voltages. Period of CBO is the same for both samples ( $10 \text{ mV} \pm 1 \text{ mV}$ ) and does not depend on gate voltages as expected for a strongly doped electron island located between the gates.

both  $V_{g1}$  and  $V_{g2}$ . Nearly equal periods measured in  $V_{g1}$  and  $V_{g2}$  means that the Coulomb island sits between the gates. This gives a coupling capacitance between the central dot and each gate of 16 aF, in good agreement with an estimation based on the geometry. This capacitance is smaller than that between a MOS-SET and its covering gate, of about 40 aF<sup>1</sup>.

CBO exist only if the conductance of both silicon nanowires below the gates are small enough to confine the electrons. Increasing one gate voltage (for instance  $V_{g2}$  in Fig. 4) suppresses CBO. This is expected because the charge is not a good quantum number as soon as one of the two barriers is sufficiently transparent. Fig. 4 shows how CBO evolve with the increase of conductance of barrier 2. At  $V_{g2} = -700$  mV barrier 2 is more resistive than 1 and dominates the total conductance, leading to constant-height oscillations. At  $V_{g2} = -550$  mV modulation of peak height arises from the dependence of barrier 1 transparency with  $V_{g1}$ . The contrast of CBO is progressively reduced as the increased coupling to electrode 2 decreases the charging energy and co-tunneling is favored ( $V_{g2} = -150$  mV). At  $V_{g2} = 250$  mV only the aperiodic pattern, similar to that shown on Fig. 2, remains.

The technique of forming quantum dots by implantation between top gates acting as a blanket mask can easily be extended to create coupled dots. Sample with three gates provides fully tunable double quantum dot (see Fig. 5). For this sample smaller gate lengths are used (40 nm, in Fig. 1) and the external gates partially cover the nanowire. Therefore greater negative gate voltage  $V_{g1}$  and  $V_{g2}$  has to be applied to deplete nanowire below the gates. Varying  $V_{g3}$  on the central gate permits two quantum dots with various inter capacitive coupling to merge into a single bigger dot<sup>10</sup>.

The gate capacitances of our coupled As-implanted quantum dot are larger than those of its intrinsic silicon analogue<sup>4</sup>. This reflects the smaller gate oxide thickness used in our case (5 nm instead of 30 nm), not a difference in sizes which are indeed comparable. In particular the

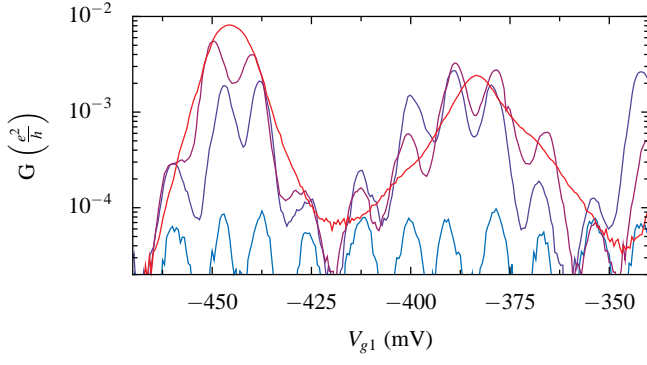


FIG. 4. Drain-source conductance versus  $V_{g1}$  at various  $V_{g2}$  at 4.2 K for a double gate sample with  $L_g = 40$  nm.  $V_{g2} = -700$  mV (light blue),  $-550$  mV (dark blue),  $-150$  mV (violet),  $250$  mV (red). For low  $V_{g2}$  the current is limited mainly by the barrier 2. At large  $V_{g2}$  CBO are suppressed by strong coupling to the drain through barrier 2. The enveloping structure is due to gate modulation of the tunneling transmission under gate 1. The shift towards positive  $V_{g1}$  with decreasing  $V_{g2}$  due to the cross talking between gates has been subtracted.

capacitance between the merged island and central gate 3 is  $C_{g3} = 24.2$  aF instead of  $C_{LGC} = 6.7$  aF in Ref. 4.

In conclusion we have made fully tunable coupled silicon quantum dots by local implantation of As in a silicon nanowire for the first time. The chemical doping permits a high lateral gradient of concentration and a compact silicon dot with a high carrier number and excellent FET control of the tunnel barriers. The in-and-out tunneling rates as well as the interdot coupling are fully controllable by top gates. The design is particularly attractive for building an electron pump.

The research leading to these results has received funding from the European Community's seventh Framework (FP7 2007/2013) under the Grant Agreement Nr:214989. The samples subject of this work have been designed and made by the AFSID Project Partners <http://www.afsid.eu>.

- <sup>1</sup>M. Pierre, R. Wacquez, B. Roche, X. Jehl, M. Sanquer, M. Vinet, E. Prati, M. Belli, and M. Fanciulli, *Appl. Phys. Lett.* **95**, 242107 (2009).
- <sup>2</sup>M. Hofheinz, X. Jehl, M. Sanquer, G. Molas, M. Vinet, and S. Deleonibus, *Appl. Phys. Lett.* **89**, 143504 (2006).
- <sup>3</sup>M. Hofheinz, X. Jehl, M. Sanquer, G. Molas, M. Vinet, and S. Deleonibus, *Eur. Phys. J. B* **54**, 299 (2006).
- <sup>4</sup>A. Fujiwara, H. Inokawa, K. Yamazaki, H. Namatsu, Y. Takahashi, N. M. Zimmerman, and S. B. Martin, *Appl. Phys. Lett.* **88**, 053121 (2006).
- <sup>5</sup>T. M. Buehler, V. Chan, A. J. Ferguson, A. S. Dzurak, F. E. Hudson, D. J. Reilly, A. R. Hamilton, R. G. Clark, D. N. Jamieson, C. Yang, C. I. Pakes, and S. Praver, *Appl. Phys. Lett.* **88**, 192101 (2006).
- <sup>6</sup>M. Mitic, M. C. Cassidy, K. D. Petersson, R. P. Starrett, E. Gauja, R. Brenner, R. G. Clark, A. S. Dzurak, C. Yang, and D. N. Jamieson, *Appl. Phys. Lett.* **89**, 013503 (2006).
- <sup>7</sup>V. C. Chan, T. M. Buehler, A. J. Ferguson, D. R. McCamey, D. J. Reilly, A. S. Dzurak, and R. G. Clark, *J. Appl. Phys.* **100**, 106104 (2006).

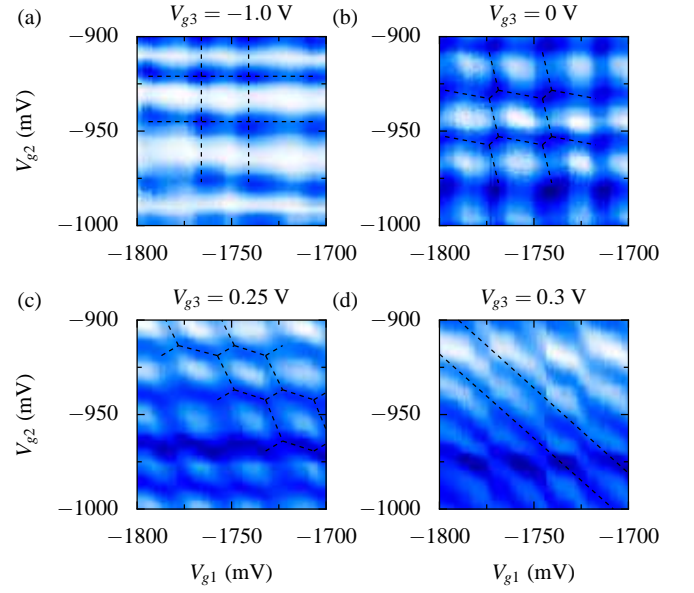


FIG. 5. Color plot of the drain-source conductance in a triple gate sample at 4.2 K. The panels correspond to different values of the gate voltage  $V_{g3}$  applied to the central gate.  $V_{g1}$  and  $V_{g2}$  are both strongly negative to isolate the double dot from source and drain. The color scale is arbitrary (blue means high conductance: maximum is  $0.006 e^2/h$  for panel (a) and  $0.12 e^2/h$  for the others). Dashed lines are guides for the eyes. (a) Capacitance coupling between the two dots is negligible. The points at which both dots are non-blockaded are on a square lattice. The lines joining these points are due to cotunneling. (b) Inter-dot capacitive coupling is increased. The points on the square lattice are extended along the diagonal. (c) A clear honeycomb pattern is observed, characteristic of a strongly capacitively coupled double dot system. (d) The anti-diagonal pattern of lines indicates the formation of a single big dot.

- <sup>8</sup>S. J. Angus, A. J. Ferguson, A. S. Dzurak, and R. G. Clark, *Appl. Phys. Lett.* **92**, 112103 (2008).
- <sup>9</sup>A. Fujiwara, N. M. Zimmerman, Y. Ono, and Y. Takahashi, *Appl. Phys. Lett.* **84**, 1323 (2004).
- <sup>10</sup>H. Liu, T. Fujisawa, H. Inokawa, Y. Ono, A. Fujiwara, and Y. Hirayama, *Appl. Phys. Lett.* **92**, 222104 (2008).
- <sup>11</sup>K. Y. Tan, K. W. Chan, M. Möttönen, A. Morello, C. Yang, J. van Donkelaar, A. Alves, J.-M. Pirkkalainen, D. N. Jamieson, R. G. Clark, and A. S. Dzurak, *Nano Lett.* **10** (1), 11 (2010).
- <sup>12</sup>A. Morello, C. C. Escott, H. Huebl, L. H. Willems van Beveren, L. C. L. Hollenberg, D. N. Jamieson, A. S. Dzurak, and R. G. Clark, *Phys. Rev. B* **80**, 081307(R) (2009).
- <sup>13</sup>Y. Ono, K. Nishiguchi, A. Fujiwara, H. Yamaguchi, H. Inokawa, and Y. Takahashi, *Appl. Phys. Lett.* **90**, 102106 (2007).
- <sup>14</sup>G. P. Lansbergen, R. Rahman, C. J. Wellard, I. Woo, J. Caro, N. Collaert, S. Biesemans, G. Klimeck, L. C. L. Hollenberg, and S. Rogge, *Nature Phys.* **4**, 656 (2008).
- <sup>15</sup>M. Pierre, R. Wacquez, X. Jehl, M. Sanquer, M. Vinet, and O. Cueto, *Nature Nanotech.* **5**, 133 (2010).
- <sup>16</sup>T. Schenkel, A. Persaud, S. J. Park, J. Nilsson, J. Bokor, J. A. Liddle, R. Keller, D. H. Schneider, D. W. Cheng, and D. E. Humphries, *J. Appl. Phys.* **94**, 7017 (2003).
- <sup>17</sup>M. Hofheinz, X. Jehl, M. Sanquer, G. Molas, M. Vinet, and S. Deleonibus, *Phys. Rev. B* **75**, 235301 (2007).